JOURNAL OF WATER AND LAND DEVELOPMENT

Land cover change detection in northwestern Vietnam using Landsat images and Google Earth Engine

Luong B. NGUYEN ✉

Thuyloi University, Faculty of Water Resource Engineering, 175 Tay Son, Dong Da, Hanoi 100000, Vietnam

Abstract

Recently, Google Earth Engine (GEE) provides a new way to effectively classify land cover utilizing available in-built classifiers. However, there have a few studies on the applications of the GEE so far. Therefore, the goal of this study is to explore the capacity of the GEE platform in terms of land cover classification in Dien Bien Province of Vietnam. Land cover classification in the year of 2003 and 2010 were performed using multiple-temporal Landsat images. Two algorithms – GMO Max Entropy and Classification and Regression Tree (CART) integrated into the Google Earth Engine (GEE) platform – were applied for this classification. The results indicated that the CART algorithm performed better in terms of mapping land use. The overall accuracy of this algorithm in the year of 2003 and 2010 were 80.0% and 81.6%, respectively. Significant changes between 2003 and 2010 were found as an increase in barren land and a reduction in forest land. This is likely due to the slash-and-burn agricultural practice of ethnic minorities in the province. Barren land seems to occur more at locations near water sources, reflecting the local people's unsuitable farming practice. This study may provide useful information in land cover change in Dien Bien Province, as well as analysis mechanisms of this change, supporting environmental and natural resource management for the local authorities.

Key words: *cloud-based platform, deforestation, land cover classification, satellite images*

INTRODUCTION

Land cover information over large areas is of paramount importance for various resources management, policy purposes and human activities [CIHLAR 2000; KAUR *et al.* 2019; MOHAMMADI *et al.* 2019; VOGELMANN *et al.* 2017; ZURQANI *et al.* 2018]. Changes in land cover have paid attention as the essential factors of global environment and sustainability studies [LIU, YANG 2015; NOSZCZYK 2019]. These changes come from different variables, including socio-economic, environmental, political, technological, and cultural condition [NOSZCZYK *et al.* 2017]. Statistical-based modelling is a common approach to assess changes in land cover [NOSZCZYK *et al.* 2017; NOSZCZYK *et al.* 2020]. However, this method only provides the change in temporal but not in spatial scale. In addition, it requires multiple-years land cover databases, which may not available in many regions, typically in developing countries.

In recent years, remotely sensed data provide a wealth of information for land cover change, due to its broad coverage in both temporal and spatial scales [GROSS *et al.* 2013; SIDHU *et al.* 2018]. However, land cover classification from satellite imagery is often complex. A common procedure for land cover classification using satellite images is: (1) download satellite images from online storage (e.g., USGS Earth Explorer, Copernicus Open Access Hub, NASA Earth Data Search); (2) import these satellite images into a GIS or remote sensing software (e.g., ArcGIS, ERDAS); (3) merge multiple images in to one image if it has more than one images covering the case study; (4) classify land cover using available plugins in the merged image of the step (3) [JENSEN 2015; PIMPLE *et al.* 2018].

In 2010, Google launched a platform called Google Earth Engine (GEE) [USGS 2010], which retains a freely accessed 40 years of historical satellite imagery. In addition, the GEE provides many advanced land cover classification algorithms [HU, HU 2019; NYLAND *et al.* 2018].

Therefore, this platform offers a new way to effectively classify land cover utilizing available in-built classifiers and satellite imagery in it.

Given the above factors, the goal of this study is to assess land cover change in Dien Bien Province of northwestern Vietnam, using the GEE platform. Being to do that, this study classified land cover in the given study in two years 2003 and 2010. Then, the changes in land cover between these years were analyzed. This study selected the Dien Bien Province as a case study because during the last decades, it has undergone a great many modifications in land cover, specifically in forest land. It is reported that deforestation rate in this province is the highest rate in the country [LE *et al.* 2018]. However, there is a little information on spatial land cover in this area. Land cover classification from the GEE is worthy for such area to better understand its land changes over time.

MATERIALS AND METHODS

CASE STUDY

Dien Bien is a mountainous province located in northwestern Vietnam that borders Laos and China (Fig. 1). The total area of this province is 956,290 ha, with significant variation in elevation, from 137 m to 2184 m. The elevation information was derived from 90 m Shuttle Radar Topography Mission (SRTM) (https://www2.jpl.nasa.gov/srtm/). The total population is 512,300 (2011 figure, General Statistics Office of Vietnam), with 21 ethnic groups.
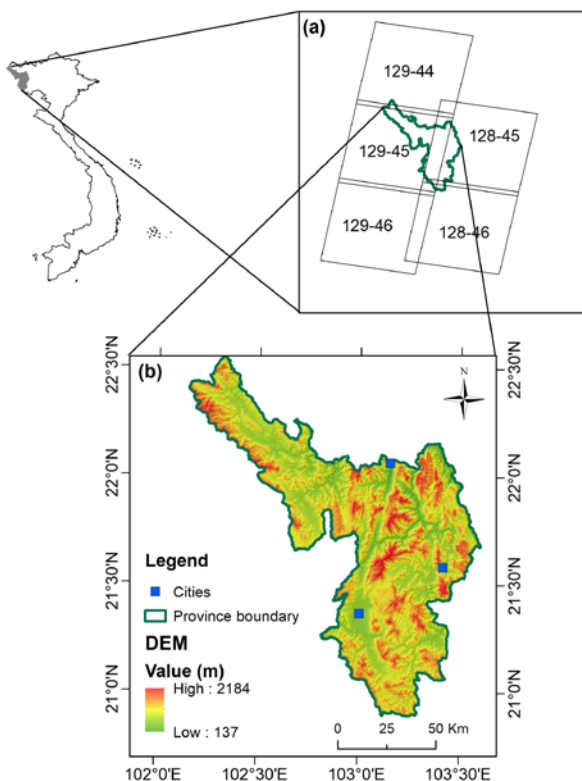

Fig. 1. Study area Dien Bien Province with (a) LANDSAT scenes cover, figure in each scene denotes path-row; and (b) Digital Elevation Model; source: own elaboration

The province is affected by a tropical monsoon with two distinct seasons: the dry season (November–April) and the wet season (May–October) [TRAN *et al.* 2012]. The province's primary economic development consists of agricultural production, livestock farming, forest exploitation, and tourist activities [TRUONG 2017]. Land-use changes in this region are due to forest plantation, agricultural expansion, hydropower construction, and urbanization [HOANG *et al.* 2017].

SAMPLING DATA

Ground truth data for land cover classification training and verification was collected through Google Earth, Google Street View, and Open Street Map using a visual interpretation. The reasons to select these sources are (1) freely accessible; (2) consist of high-quality images; (3) suggested by previous studies [DUONG *et al.* 2018]. This study used them to cross-check the sampling results from others. The homogenous area of those reference objects must be more than 20 m in diameter [DUONG *et al.* 2018]. It can ensure the homogeneity of training samples which reduce the chance in false land cover detection later. Based on local knowledge, this study categorized land cover into six groups, including forest; build-up area; cropland; paddy rice; barren land; and water. Illustration examples for each category can be seen in Figure 2. In total, this study collected a total of 1489 reference data points in 2003, and 1801 reference data points in 2010 (Fig. 3).

LAND COVER CLASSIFICATION WITH GOOGLE EARTH ENGINE

Figure 4 presents a flow chart to classify land cover from Landsat data using the supervisor training method. The less-cloudy, multiple-temporal Landsat images for the selected years (2003 and 2010), were collected and merged over the case study. It is ideal that the imagery used for land cover detection is free of clouds. However, there always have substantial amount of water vapor in the atmosphere resulting in high relative humidity or haze in certain areas in the atmosphere. These mediums can cause a false land cover detection from the satellite imagery and therefore, it is essential to mark cloudy areas [JENSEN 2015]. This study used simple Composite algorithm in Earth Engine library to reduce the effect of cloud. From multiple temporal images, this algorithm selected the lowest possible range of cloud scores at each point and then computed per-band percentile values from the accepted pixels.

There are five Landsat scenes with path-row numbers as 128-45, 128-46, 129-44, 129-45, 129-46. Details can be found at Figure 1a. In 2003, a total of 24 images were collected and these figures in 2010 were 48 images. Details of selected images can be found in Table 1. The selection has automatically done in the GEE platform. It can be seen that more images during the dry season (November–April) were obtained that these images during the wet season (May–October). This is because that in the dry season, there are more chances to get less-cloudy imagery than in the wet season.

Forest   Built-up area   Cropland

Paddy rice   Barren land   Water
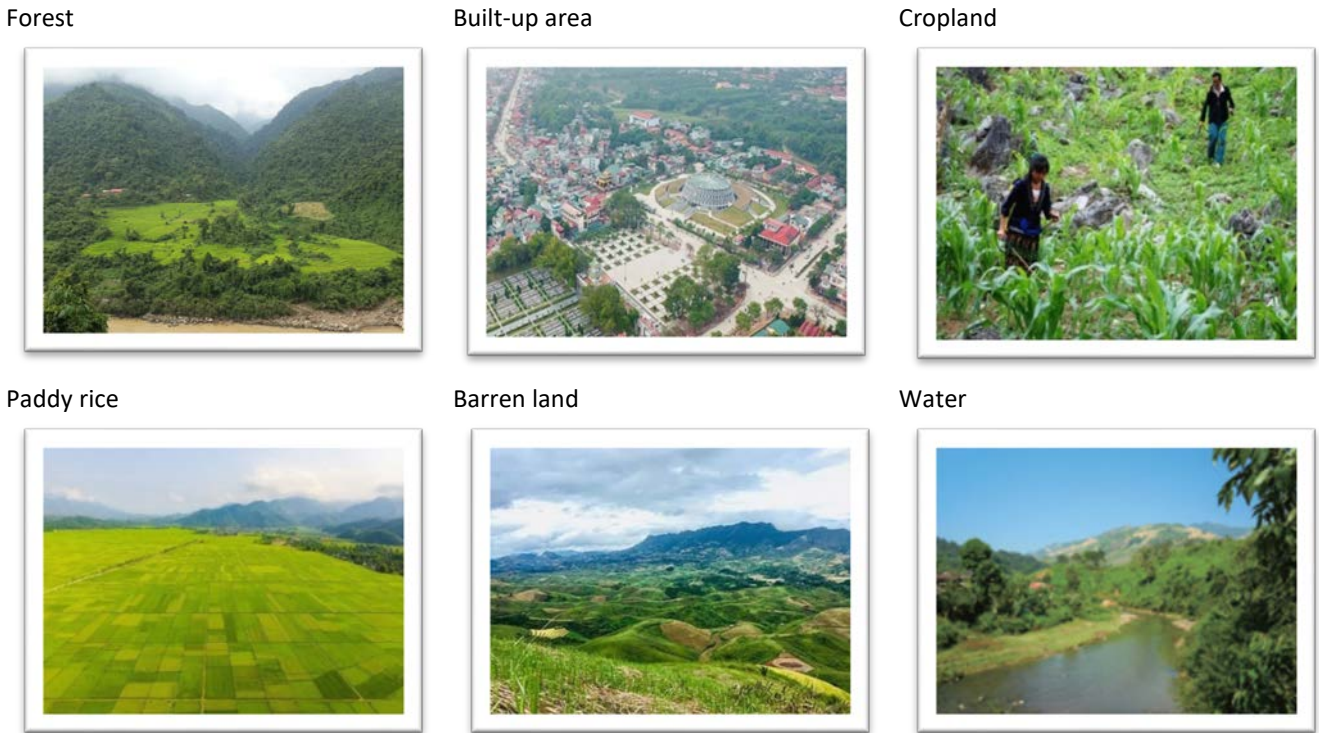
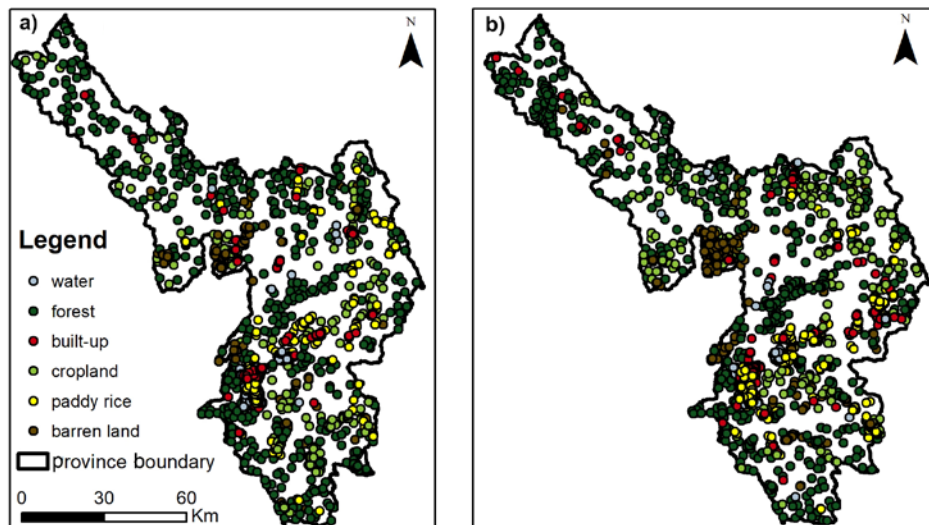Fig. 2. Different land cover type in the case study; sources: the author, Google Earth and JICA [2016]

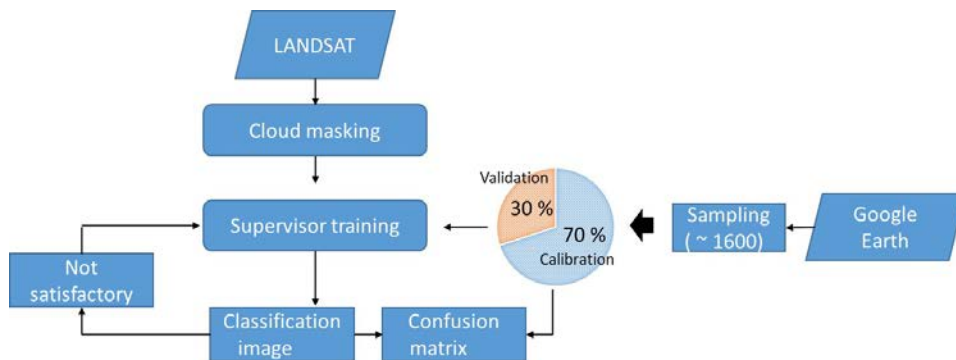Fig. 3. Distribution of reference data in two years: a) 2003, b) 2010; source: own study

Fig. 4. Flow chart of land cover classification; source: own elaboration

Table 1. Selected Landsat imagery for land cover classification in 2003 and 2010 in Dien Bien Province

LANDSAT scenes (path-row)	2003		2010	
	n	date (mm/dd)	n	date (mm/dd)
128-45	10	01/12, 03/01, 04/02, 04/18, 05/04, 09/25, 10/27, 11/12, 12/14, 12/30	11	01/15, 01/31, 02/16, 03/20, 04/05, 04/21, 09/12, 09/28, 10/30, 11/15, 12/17
128-46	8	01/12, 02/13, 03/01, 04/02, 09/25, 10/27, 12/14, 12/30	7	01/15, 01/31, 02/16, 03/20, 04/21, 09/28, 10/30
129-44	2	11/19, 12/05	12	01/22, 02/07, 02/23, 04/12, 04/28, 05/14, 07/17, 09/19, 10/21, 11/06, 11/22, 12/24
129-45	2	11/19, 12/05	10	01/22, 02/07, 02/23, 03/27, 04/28, 05/14, 07/17, 09/03, 11/06, 12/24
129-46	2	11/19, 12/05	8	02/07, 02/23, 03/27, 04/28, 05/14, 09/03, 11/06, 12/24
Total	**24**		**48**	

Explanations: *n* = total samples.
Source: own elaboration.

This study selected two built-in classifiers in the GEE – GMO Maximum Entropy and Classification and Regression Tree (CART) for classifying land cover in the case study. These classifiers are all supervised classification, which is to be provided pre-defined "reference data" – areas are known to be representation of homogenous examples of land cover types. The classifiers are trained with the spectral characteristics of these known areas. Various statistical parameters, including means, standard deviations, covariance metrics, are estimated for each training site. Every pixel located in- and out-side the reference sites then evaluated and assigned to the land cover category which it has the highest likelihood to be [JENSEN 2015]. The GMO Maximum Entropy is a multinomial logistic regression classifier that is a generalization of linear regression using the softmax transformation function. This classifier aims to minimize an error function by taking a negative logarithm of the likelihood, which means cross-entropy [MCDONALD *et al.* 2009]. The CART is a binary decision tree classifier with logical if-then questions, building in a concept of information entropy. In this technique, the input data is randomly divided into certain of nodes. In each node, one attribute of the data that most effectively splits its set of samples into subsets enriched in one class or other is selected [BREIMAN *et al.* 1984]. The GMO Maximum Entropy and the CART were performed in the GEE with Classifier.gmoMaxEnt and Classifer.cart available in Earth Engine library, respectively.

The calibration process was performed on 70% of ground truth data, then the classification maps were evaluated by the confusion matrix with the rest of the 30% reference data. In order to evaluate the performances of land cover classification, this study used overall accuracy, producer's accuracy, and user's accuracy based on a confusion matrix [JENSEN 2015]. These metrics formulas are as follows:

$$OA = \frac{\sum_{i=1}^{k} x_{ii}}{N} 100 \qquad (1)$$

$$PA_j = \frac{x_{jj}}{x_{+j}} 100 \qquad (2)$$

$$UA_i = \frac{x_{ii}}{x_{i+}} 100 \qquad (3)$$

Where: *OA*, *PA_j*, *UA_i* are overall accuracy, producer's accuracy for class *j*, user's accuracy for class *i*, respectively; x_{ii} = the number of observations in row *i* and column *i* of the confusion matrix; x_{i+}, x_{+j} = the marginal total of row *i* and column *j*, respectively; *N* = the total number of samples.

The overall accuracy of the classification map is a percentage of corrected classified pixels to the total number of pixels in the confusion matrix. The producer's accuracy is a percentage of corrected classified pixels in a class, to the total number of pixels of that class as determined from the ground truth data (the column total of the confusion matrix). The user's accuracy is a percentage of corrected classified pixels in a class to the total number of pixels that were actually classified in that category (the row total of the confusion matrix).

RESULTS AND DISCUSSION

LAND COVER LAND CLASSIFICATION

Table 2 presents the performances of CART and GMO Maximum Entropy, with validation data in 2003 and 2010. The overall accuracy values indicated a slightly better performance of CART to GMO Maximum Entropy, which is in line with FARDA [2017] and SHELESTOV *et al.* [2017]. Therefore, further detail analysis of the confusion matrix and land cover change detection between 2003 and 2010 were made based on the results from the CART algorithm.

Table 2. Comparison performance of CART and GMO Maximum Entropy (OA metric) on land cover classification for calibration data set

Year	Overall accuracy	
	GMO Maximum Entropy	CART
2003	78.2	80.0
2010	79.6	81.6

Source: own study.

Table 3 presents the confusion matrix and accuracy assessment for land cover classification in the year 2003 and 2010. According to PLOURDE and CONGALTON [2003], a minimum of 50 samples per land cover class are recommended. In this study, apart from water, samples of other land cover categories were over 50, ensuring the minimum requirement of the sample sizes.

Generally, the user accuracy exhibited better scores than the producer accuracy, demonstrating that the CART algorithm could meet the general rule of land cover classification, where it is better to leave some pixels unclassified (producer errors) rather than to have large numbers of user errors (assigning a pixel to a class to which it does not belong) [JENSEN 2015]. The classification for urban, cropland

Table 3. Confusion matrix of land cover classification in 2003 using CART

Specification		Ground truth						Row total	PA (%)
		water	forest	urban	crop land	rice paddy	barren		
2003									
Image	water	33	2	1	0	1	0	37	89.2
	forest	1	114	1	4	3	3	126	90.5
	urban	0	0	44	2	15	0	61	72.1
	crop land	0	5	7	35	3	10	60	58.3
	rice paddy	0	1	2	11	66	2	82	80.5
	barren	0	6	4	3	0	56	69	81.2
Column total		34	128	59	55	88	71	435	78.6
UA (%)		97.1	89.1	74.6	63.6	75.0	78.9	79.7	80.0
2010									
Image	water	45	0	0	0	3	0	48	93.8
	forest	0	145	1	1	2	11	160	90.6
	urban	0	0	54	4	7	1	66	81.8
	crop land	0	7	2	47	5	14	75	62.7
	rice paddy	2	3	3	6	69	1	84	82.1
	barren	0	6	1	15	4	78	104	75.0
Column total		47	161	61	73	90	105	537	81.0
UA (%)		95.7	90.1	88.5	64.4	76.7	74.3	81.6	81.6

Explanations: PA = producer accuracy, UA = user accuracy.
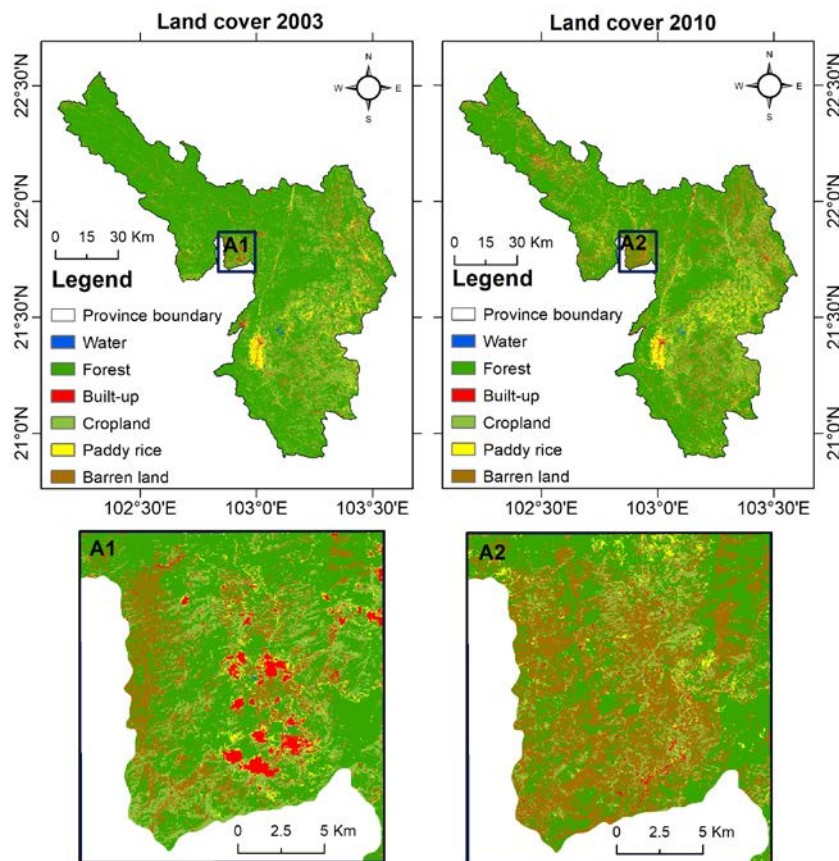Source: own study.

Fig. 5. Land cover classification in 2003 and 2010; panel A1 and A2 are zoom in of land cover in 2003 and 2010, respectively; source: own study

and barren lands exhibited low scores in both user accuracy and producer accuracy. The urban land is often skewed with high variation; therefore, it is challenging to predict this. The low performances with regard to cropland and barren land were due to these two classes being often mixed in this case study.

LAND COVER CHANGE DETECTION

The land cover classifications using the CART algorithm, in 2003 and 2010, are illustrated in Figure 5. It can be seen that forest land covers almost Dien Bien Province. However, in the northwest of the province, there was a sig-

Table 4. Land cover change matrix between 2003 and 2010 in Dien Bien Province

2003	2010							
	water	forest	urban	cropland	rice paddy	barren	total (ha)	total (%)
Water	**1,424**	340	44	75	505	21	2,409	0.3
Forest	154	**540,916**	3,428	49,609	37,372	54,307	685,787	71.7
Urban	264	3,005	**1,903**	4,281	1,803	2,485	13,741	1.4
Cropland	83	35,237	3,734	**62,047**	14,762	42,576	158,439	16.6
Rice paddy	632	12,532	2,182	8,841	**22,386**	2,887	49,461	5.2
Barren	9	9,109	735	15,925	1,698	**18,976**	46,453	4.9
Total (ha)	2,567	601,140	12,025	140,779	78,526	121,253	**956,290**	100.0
Total (%)	0.3	62.9	1.3	14.7	8.2	12.7	100.0	

Explanations: bold values denote unchanged areas (ha).
Source: own study.

nificant change as built-up area and crop land were replaced by barren land. Table 4 presents land cover change matrix between 2003 and 2010. Two major changes were an increase in barren land and a reduction in forest land. In 2003, barren land accounted for only 4.9% (46,453 ha) of total land. In 2010, this figure increased to 12.7% (121,253 ha). On the contrary, forest land experienced a significant decline of 8.9%, from 71.7% (685,787 ha) to 62.9% (601,140 ha) of the total area in 2003 and 2010, respectively. The forest loss mainly was due to a conversion to barren land (54,307 ha), followed by cropland (49,609 ha), and rice paddy (37,372 ha). At the same time, other land uses also converted to forest. For example, 35,237 ha of cropland was converted to forest, followed by rice paddy (12,532 ha).

BARREN LAND PROBLEM IN DIEN BIEN PROVINCE

According to land use change analysis at the previous section, barren land has increased dramatically during 2003 to 2010. This is in agreement with previous studies [JICA 2016]. Barren land may be caused by (1) cut trees for households and wood processing businesses [KIEN, HARWOOD 2017], or (2) slash-and-burn agricultural activities [MEYFROIDT, LAMBIN 2008]. These slash-and-burn agricultural activities are more pronounced than logging activities in terms of increasing barren land [JICA 2016]. That unsuitable farming practice is mainly taken by ethnic minorities living in the province. They burn forests on high mountainous areas in order to grow crops (cropland). After several years, due to their limitations in technological cultivation, the crop-growing lands begin degradation, resulting in a reduction in crop quality [MEYFROIDT, LAMBIN 2008]. Those ethnic minorities then move to other sites to renew their cycle of burning forest, growing cropland, and leaving it as relatively low-nutrition land. The cropland with land degradation is afterward classified as barren land. The slash-and-burn agricultural activities affects not only deforestation but also loss of habitat and species; a reduction in air quality; an increase in accidental fires; a risk of soil erosion; and the loss of beautiful mountain landscapes. This study highlights the last consequence, because eco-tourism is one source of incomes for Dien Bien Province.

Predicting barren land due to slash-and-burn agriculture is of extreme importance. Since ethnic groups are not

well educated, we assume their habits are somehow associated with natural conditions, with relatively poor cultivation methods and using water primarily from rainfall and natural watercourses for their crop growing lands. The barren lands were categorized in different groups, which takes into account the distance of these lands to watercourses (creeks, rivers, lakes, reservoirs). This study found that barren land likely occurred among the groups closing to the watercourses (0–1,500 m). After 1,500 m, barren land exhibited a significant reduction (Fig. 6). This finding proved water is one of the essential factors for the movement of ethnic minorities.
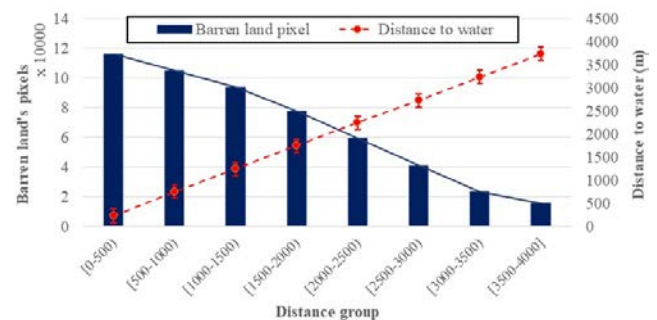

Fig. 6. Relationship between barren land and distance to water course; source: own study

LIMITATION AND FURTHER STUDY

This study has limitations in identifying sampling data. Normally, these sites require field trips to collect. However, considering the complexity of the study area as well as human resource constraints, this study obtained the sampling data through remoted tools, including Google Earth, Google Street View, and Open Street Map.

Further studies can classify more land cover in different years, creating land cover database for the given study. This will help on land cover modelling and land cover trend assessment [NOSZCZYK 2019]. Regarding barren land due to the movement of ethnic minorities, other factors may affect to this movement, including soil properties, slopes, topography, and weather conditions. Further studies could investigate on these factors. It can benefit to build regression models to predict barren land due to the unsuitable farming practice of ethnic minorities.

CONCLUSIONS

1. The GMO Maximum Entropy and CART algorithms integrated into the Google Earth Engine (GEE) platform were applied for land cover classification, with the slightly better performance granted to the latter one. The overall accuracy of the CART algorithms in the years of 2003, and 2010 were 80.0% and 81.6%, respectively.

2. Urban land, cropland, and barren land exhibited poor quality in classification. This is because urban is hard to predict, while cropland and barren land are often mixed in the case study.

3. Major changes between 2003 and 2010 were found as an increase in barren land and a reduction of forest land. This is likely due to the slash-and-burn agricultural practice of ethnic groups in the province. Water resources may be an important factor to note in models, to predict barren land due to the poor agricultural habits of these ethnic groups.

This study exhibits the capacity of the GEE in classifying land cover. This platform has great advantage in high computationally efficiency. Raw satellite imagery datasets are already available on the GEE servers so that there is no need to download such huge amount of data. This is beneficial to scientists from developing countries where local resources (computer, commercial software) are limited.

REFERENCES

BREIMAN L., FRIEDMAN J., STON C.J., OLSHEN R.A. 1984. Classification and regression trees. CRC Press. ISBN 0412048418 pp. 368.

CIHLAR J. 2000. Land cover mapping of large areas from satellites: status and research priorities. International Journal of Remote Sensing. Vol. 21. Iss. 6–7 p. 1093–1114. DOI 10.1080/014311600210092.

DUONG P., TRUNG T., NASAHARA K., TADONO T. 2018. JAXA High-resolution land use/land cover map for central Vietnam in 2007 and 2017. Remote Sensing. Vol. 10. Iss. 9, 1406. DOI 10.3390/rs10091406.

FARDA N. 2017. Multi-temporal land use mapping of coastal wetlands area using machine learning in Google Earth En-gine. In: IOP Conference Series: Earth and Environmental Science (GSS 2017). 27–28.09.2017 Yogyakarta, Indonesia. IOP Publishing. Vol. 98, 012042. DOI 10.1088/1755-1315/98/1/012042.

GROSS D., DUBOIS G., PEKEL J.-F., MAYAUX P., HOLMGREN M., PRINS H.H.T., RONDININI C., BOI-TANI L. 2013. Monitoring land cover changes in African protected areas in the 21st century. Ecological Informatics. Vol. 14 p. 31–37. DOI 10.1016/j.ecoinf.2012.12.002.

HOANG T.T., NASAHARA K.N., KATAGI J. 2017. Analysis of land cover changes in northern Vietnam using high resolution remote sensing data. In: Advances and applications in geospatial technology and Earth resources. Proceedings of the Inter-national Conference on Geo-Spatial Technologies and Earth Resources. Springer p. 134–151.

HU Y., HU Y. 2019. Land cover changes and their driving mechanisms in Central Asia from 2001 to 2017 supported by Google Earth Engine. Remote Sensing. Vol. 11. Iss. 5, 554. DOI 10.3390/rs11050554.

JENSEN J.R. 2015. Introductory digital image processing: A remote sensing perspective. 4th ed. Pearson Series in Geographic Information Science. ISBN 013405816X pp. 656.

JICA 2012. Potential forests and land related to climate change and forest in Vietnam. Hanoi, Vietnam. Vietnam National University of Forestry pp. 129 [in Vietnamese].

JICA 2016. Forest can change the world. Japan International Cooperation Agency pp. 16.

KAUR A., GHOSH S., DAS S.K. 2019. Satellite image-based land use/land cover dynamics and forest cover change analysis (1996–2016) in Odisha, India. Asian Journal of Water, Environment and Pollution. Vol. 16. Iss. 1 p. 25–39. DOI 10.3233/FAOAJW190004.

KIEN N.D., HARWOOD C. 2017. Timber demand and supply in northwest Vietnam: The roles of natural forests and planted trees. Small-scale Forestry. Vol. 16. Iss. 1 p. 65–82. DOI 10.1007/s11842-016-9343-0.

LE T.H., THANH L.Q., DANG T.T., TRAN L.D., ZIMMER H., NICHOLS J.D. 2018. Forest rehabilitation options and sus-tainable management plans for northwest Vietnam. APFNet Training Workshop. Yunnan, China pp. 90.

LIU T., YANG X. 2015. Monitoring land changes in an urban area using satellite imagery, GIS and landscape metrics. Applied Geography. Vol. 56 p. 42–54. DOI 10.1016/j.ejrs.2016.08.002.

MCDONALD R., MOHRI M., SILBERMAN N., WALKER D., MANN G.S. 2009. Efficient large-scale distributed training of conditional maximum entropy models. In: Advances in Neural Information Processing Systems 22 (NIPS 2009). Eds. Y. Bengio, D. Schuurmans, J.D. Lafferty, C.K.I. Williams, A. Culotta p. 1231–1239.

MEYFROIDT P., LAMBIN E.F. 2008. The causes of the reforestation in Vietnam. Land Use Policy. Vol. 25(2) p. 182–197. DOI 10.1016/j.landusepol.2007.06.001.

MOHAMMADI A., SHAHABI H., BIN AHMAD B. 2019. Land-cover change detection in a part of Cameron Highlands, Malaysia using ETM+ Satellite imagery and Support Vector Machine (SVM) Algorithm. Environment Asia. Vol. 12. Iss. 2 p. 145–154. DOI 10.14456/ea.2019.36.

NOSZCZYK T. 2019. A review of approaches to land use changes modeling. Human and Ecological Risk Assessment: An International Journal. Vol. 25. Iss. 6 p. 1377–1405. DOI 10.1080/10807039.2018.1468994.

NOSZCZYK T., RUTKOWSKA A., HERNIK J. 2017. Determining changes in land use structure in Małopolska using statistical methods. Polish Journal of Environmental Studies. Vol. 26. Iss. 1 p. 211–220. DOI 10.15244/pjoes/64913.

NOSZCZYK T., RUTKOWSKA A., HERNIK J. 2020. Exploring the land use changes in eastern Poland: Statistics-based modeling. Human and Ecological Risk Assessment: An International Journal. Vol. 26. Iss. 1 p. 255–282. DOI 10.1080/10807039.2018.1506254.

NYLAND K.E, GUNN G.E., SHIKLOMANOV N.I., ENG-STROM R.N., STRELETSKIY D.A. 2018. Land cover change in the lower Yenisei River using dense stacking of landsat imagery in Google Earth Engine. Remote Sensing. Vol. 10(8), 1226. DOI 10.3390/rs10081226.

PIMPLE U., SIMONETTI D., SITTHI A., PUNGKUL S., LEADPRATHOM K., SKUPEK H., SOM-ARD J., GOND V., TOWPRAYOON S. 2018. Google Earth engine based three decadal landsat imagery analysis for mapping of mangrove forests and its surround-

ings in the Trat province of Thailand. Journal of Computer and Communications. Vol. 6. Iss. 1 p. 247–264. DOI 10.4236/jcc.2018.61025.

Plourde L., Congalton R.G. 2003. Sampling method and sample placement. Photogrammetric Engineering and Remote Sensing. Vol. 69. Iss. 3 p. 289–297.

Shelestov A., Lavreniuk M., Kussul N., Novikov A., Skakun S. 2017. Exploring Google Earth engine plat-form for big data processing: Classification of multi-temporal satellite imagery for crop mapping. Frontiers in Earth Science. Vol. 5, 17. DOI 10.3389/feart.2017.00017.

Sidhu N., Pebesma E., Câmara G. 2018. Using Google Earth Engine to detect land cover change: Singapore as a use case. European Journal of Remote Sensing. Vol. 51. Iss. 1 p. 486–500. DOI 10.1080/22797254.2018.1451782.

Tran T.X., Hoang M.T., Tran H.T., Nguyen K.D. 2012. Water resources on Vietnam's river system. Hanoi. Science and Technology Publisher House pp. 518. [In Vietnamese]

Truong C.N. 2017. Validation of the Terra-I forest loss detection products in Vietnam using Landsat-8 imagery: A case study of Dien Bien and Lam Dong Provinces. Clark University. MSc Thesis pp. 140.

USGS 2010. Thousands of landsat scenes in Google's Earth Engine [online]. U.S. Geological Survey. [Access 10.11.2019]. Available at: https://landsat.usgs.gov/google-earth-engine

Vogelmann J.E., Van Khoa P., Shermeyer J., Shi H., Wimberly M.C., Duong H.T. 2017. Assessment of forest degradation in Vietnam using landsat time series data. Forests. Vol. 8. Iss. 7. DOI 10.3390/f8070238.

Zurqani H.A., Post C.J., Mikhailova E.A., Schlautman M.A., Sharp J.L. 2018. Geospatial analysis of land use change in the Savannah River Basin using Google Earth Engine. International Journal of Applied Earth Observation and Geoinformation. Vol. 69 p. 175–185. DOI 10.1016/j.jag. 2017.12.006.